Research Article | Vol. 24, No. 16 | 8 Aug 2016 | OPTICS EXPRESS 17680

Optics EXPRESS

Sensitivity optimization with cladding-etched long period fiber gratings at the dispersion turning point

IGNACIO DEL VILLAR,[1,2,*] JOSE L. CRUZ,[3] ABIAN B. SOCORRO,[1,2] JESUS M. CORRES,[1,2] AND IGNACIO R. MATIAS[1,2]

[1] *Electrical and Electronic Engineering Department, Public University of Navarra, Edificio de Los Tejos, Campus de Arrosadia s/n, 31006 Pamplona, Spain*
[2] *Institute of Smart Cities, Public University of Navarra, Campus de Arrosadia s/n, 31006 Pamplona, Spain*
[3] *Department of Applied Physics and Electromagnetism, University of Valencia, Dr. Moliner 50, Burjassot 46100, Spain*
[*] *ignacio.delvillar@unavarra.es*

Abstract: This work presents a refractive index sensor based on a long period fiber grating (LPFG) made in a reduced cladding fiber whose low order cladding modes have the turning point at large wavelengths. The combination of these parameters results in an improved sensitivity of 8734 nm/refractive index unit (RIU) for the $LP_{0,3}$ mode in the 1400-1650 wavelength range. This value is similar to that obtained with thin-film coated LPFGs, which permits to avoid the coating deposition step. The numerical simulations are in agreement with the experimental results.

OCIS codes: (060.2370) Fiber optics sensors; (060.3735) Fiber Bragg gratings; (060.2430) Fibers, single-mode.

References and links

1. V. Bhatia and A. M. Vengsarkar, "Optical fiber long-period grating sensors," Opt. Lett. **21**(9), 692–694 (1996).
2. X. Shu, L. Zhang, and I. Bennion, "Sensitivity Characteristics of Long-Period Fiber Grating," J. Lightwave Technol. **20**(2), 255–266 (2002).
3. I. Del Villar, M. Achaerandio, I. R. Matías, and F. J. Arregui, "Deposition of overlays by electrostatic self-assembly in long-period fiber gratings," Opt. Lett. **30**(7), 720–722 (2005).
4. A. Cusano, A. Iadicicco, P. Pilla, L. Contessa, S. Campopiano, A. Cutolo, and M. Giordano, "Cladding mode reorganization in high-refractive-index-coated long-period gratings: effects on the refractive-index sensitivity," Opt. Lett. **30**(19), 2536–2538 (2005).
5. N. D. Rees, S. W. James, R. P. Tatam, and G. J. Ashwell, "Optical fiber long-period gratings with Langmuir-Blodgett thin-film overlays," Opt. Lett. **27**(9), 686–688 (2002).
6. I. Del Villar, I. Matías, F. Arregui, and P. Lalanne, "Optimization of sensitivity in Long Period Fiber Gratings with overlay deposition," Opt. Express **13**(1), 56–69 (2005).
7. Z. Wang, J. Heflin, R. Stolen, and S. Ramachandran, "Analysis of optical response of long period fiber gratings to nm-thick thin-film coating," Opt. Express **13**(8), 2808–2813 (2005).
8. C. S. Cheung, S. M. Topliss, S. W. James, and R. P. Tatam, "Response of fiber-optic long-period gratings operating near the phase-matching turning point to the deposition of nanostructured coatings," J. Opt. Soc. Am. B **25**(6), 897–902 (2008).
9. P. Pilla, C. Trono, F. Baldini, F. Chiavaioli, M. Giordano, and A. Cusano, "Giant sensitivity of long period gratings in transition mode near the dispersion turning point: an integrated design approach," Opt. Lett. **37**(19), 4152–4154 (2012).
10. X. Chen, K. Zhou, L. Zhang, and I. Bennion, "Dual-peak long-period fiber gratings with enhanced refractive index sensitivity by finely tailored mode dispersion that uses the light cladding etching technique," Appl. Opt. **46**(4), 451–455 (2007).
11. F. Chiavaioli, P. Biswas, C. Trono, S. Bandyopadhyay, A. Giannetti, S. Tombelli, N. Basumallick, K. Dasgupta, and F. Baldini, "Towards sensitive label-free immunosensing by means of turn-around point long period fiber gratings," Biosens. Bioelectron. **60**, 305–310 (2014).
12. M. Śmietana, M. Koba, P. Mikulic, and W. J. Bock, "Measurements of reactive ion etching process effect using long-period fiber gratings," Opt. Express **22**(5), 5986–5994 (2014).
13. P. Biswas, N. Basumallick, S. Bandyopadhyay, K. Dasgupta, A. Ghosh, and S. Bandyopadhyay, "Sensitivity enhancement of turn-around-point long period gratings by tuning initial coupling condition," IEEE Sens. J. **15**(2), 1240–1245 (2015).
14. I. Del Villar, "Ultrahigh-sensitivity sensors based on thin-film coated long period gratings with reduced diameter, in transition mode and near the dispersion turning point," Opt. Express **23**(7), 8389–8398 (2015).

#261172 http://dx.doi.org/10.1364/OE.24.017680
Journal © 2016 Received 15 Mar 2016; revised 26 May 2016; accepted 17 Jul 2016; published 26 Jul 2016

Optics EXPRESS

15. Y. Zhao, Y. Liu, C. Zhou, Q. Guo, and T. Wang, "Sensing characteristics of long-period fiber gratings written in thinned cladding fiber," IEEE J. Sens. **16**(5), 1217–1223 (2016).
16. M. Daimon and A. Masumura, "Measurement of the refractive index of distilled water from the near-infrared region to the ultraviolet region," Appl. Opt. **46**(18), 3811–3820 (2007).
17. P. R. Cooper, "Refractive-index measurements of liquids used in conjunction with optical fibers," Appl. Opt. **22**(19), 3070–3072 (1983).

1. Introduction

Long period fiber gratings consist of a periodic modulation of the core refractive index in a single mode fiber (SMF) with a much longer period than the optical wavelength. This enables a co-propagating coupling between the fundamental core mode and higher order cladding modes. Each coupling of light transmitted through the core to a specific cladding mode leads to the generation of an attenuation band in the transmission spectrum.

In 1996, it was proved that it is possible to obtain both a refractometer and a strain sensor based on the attenuation band shift as a function of refractive index and strain [1].

Since that moment, many articles have been published with the aim of increasing the sensitivity of the optical fiber devices. To this purpose, three major highlights have been achieved during the last years. The first one is the dispersion turning point (DTP). Attenuation bands experience typically either a blueshift or a redshift as the grating period increases. However, for specific periods it is possible to split the optical resonance in two bands, which respectively experience a blueshift and a redshift function of the external refractive index. Gratings in this situation (the turn dispersion point [2]) have an optimal sensitivity to physical or chemical perturbations.

A second improvement can be obtained thanks to the transition to guidance of a cladding mode in the overlay [3], a phenomenon that is usually called mode transition (MT) [4]. In order to generate the MT it is necessary to deposit a thin-film over the fiber, something that was done for the first time in 2002 [5]. Adjusting the characteristics of the thin-film (i.e. refractive index and thickness), it is possible to optimize the device sensitivity [6].

The first combination of thin-film deposition with an LPFG tuned at the DTP was done by Wang et al. [7]. After that, the sensitivity was enhanced with a thin-film optimized for MT deposited on an LPFG at DTP [8], and a record sensitivity of 9100 nm/RIU was obtained [9].

A third way of increasing the sensitivity of LPFGs is by reducing the cladding diameter, typically with an etching process [10–13], and in a recent work it has been theoretically proved that a sensitivity around 143000 nm/RIU can be attained by combining adequately the three phenomena [14]. However, the experimental fitting of the phenomena seems complicated, especially due to the high precision demanded for the deposition of the thin-film.

This work is focused on the combination of the dispersion turning point and the reduction of the cladding diameter with the purpose of obtaining a maximum sensitivity without the need of a thin-film. This permits to avoid using costly deposition machines like atomic layer deposition and the cross-sensitivity of the thin-film, in case the device is used for detection of biological or chemical purposes.

Long period fiber gratings written in 80 microns diameter fibers were etched to set the turning point of low order cladding modes at the telecommunication bands. The gratings were calibrated as refractive index sensors and the results show an improved sensitivity and a reasonable agreement with theoretical calculations.

2. Experimental setup

Gratings with period 210 μm were written in a hydrogen loaded fiber from Fibercore (product code SM125(9/80), core diameter 9 μm, cladding diameter 80 μm and NA = 0.1195). This fiber with reduced diameter permits to enhance the sensitivity of the device [15], since the tail of the cladding modes spread further in the surrounding medium. Moreover, the use of an 80 μm structure permits to induce less imperfections during the etching process than in a standard fiber with 125 μm diameter. The gratings were photoinscribed point by point with a doubled argon laser; the fibers were stored for 48 hours to allow the out-diffusion of the remaining hydrogen, hence the grating stabilization. Two gratings were written for this

Optics EXPRESS

experiment. The first one (LPFG 1) had a length of 9 mm and coupled the $LP_{0,6}$ mode at 1125nm with a resonance depth of 5.5 dB after dehydrogenation. The second one (LPFG 2) had 7.5 mm in length and exhibited a resonance of 4 dB at 1125nm. No resonances corresponding to higher order modes were observed in the wavelength range of fabrication rig. A resonance of a next lower order mode was observed at 1000nm but it could have been hardly measured because the fiber works in multimode regime at that wavelength.

The two LPFGs were subjected to the etching process. The diameter of the LPFG 1 was reduced up to the moment when $LP_{0,6}$ band at DTP was observed. To this purpose, a slow etching process was performed (the LPFG was immersed in a 10% hydrofluoric acid solution), whereas LPFG 2 was etched up to 35 μm with a faster etching process (the LPFG was immersed in 40% hydrofluoric acid – HF solution) in order to obtain the $LP_{0,3}$ DTP band.

After stopping the etching process in both fibers, the wavelength shift of the attenuation bands was monitored when immersing the sensor in different glycerol solutions. The refractive index was measured with a 30GS refractometer from Mettler Toledo Inc operating at 589.3 nm. Since the measurement range in our experiments is located in the range 1300-1700 nm, reduction in 0.012 refractive index units due to dispersion of glycol and water in the infrared region was considered [16,17].

In Fig. 1 the transmission configuration setup is depicted. It consists of a broadband source (Agilent 83437A) that launches light into one end of the fiber where the grating is written. The second end is connected to an Agilent 86140B optical spectrum analyser, which monitors the transmission spectrum.

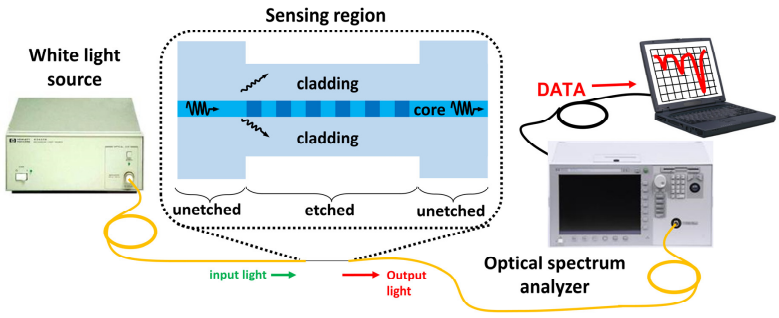

Fig. 1. Experimental setup.

3. Numerical and experimental results

In order to analyze the response of the device, and to design the gratings, we used the finite difference method FDM of FIMMWAVE® (Photon Design Inc.)

According to [14], the sensitivity progressively increases as the cladding diameter is reduced. Simultaneously, the DTP experiences a blueshift and the coupling coefficient increases (the attenuation band depth increases). In addition to this, the sensitivity increases if the DTP is located at longer wavelengths. Consequently, in order to meet all these requirements, gratings of period 210 μm and length 9 (LPFG 1) and 7.5 mm (LPFG 2) were written as it has been explained before. These period and lengths permit to observe deep attenuation bands respectively for the $LP_{0,6}$ and $LP_{0,3}$ modes at their dispersion turning points.

LPFG 1 was etched and the temporal evolution of the grating spectra is shown in Visualization 1. Measurements as a function of time were correlated with the numerical simulation as a function of the fiber diameter. The etching rate was 0.14 μm/min.

When the gratings are etched, the effective refractive index of the cladding mode decreases and the coupling wavelength shifts to larger wavelengths. Furthermore, the etching process increases the overlap between the core and the cladding mode, hence the depth of the resonance of this undercoupled gratings.

Optics EXPRESS

When etching LPFG 1, of length 9 mm, the $LP_{0,6}$ band was redshifted until the DTP was obtained at 1575 nm, as Visualization 1 shows.

After that, the LPFG 2 was progressively etched up to the turning point of the $LP_{0,3}$ coupling band. The length of the device was lower, 7.5 mm, in order to consider the progressive increase of the attenuation band depth due to coupling coefficient increase due to the diameter reduction. The evolution of the spectrum up to the $LP_{0,6}$ DTP is just the same as the one obtained with LPFG 1, except for the depth because the length of LPFG 2 is different. Also $LP_{0,5}$, $LP_{0,4}$, and $LP_{0,3}$ DTPs can be seen in Visualization 2. The etching rate, 1.25 μm/min, was higher than in LPFG 1 because 40% HF solution instead of 10% HF was used, as indicated in section 2. In Visualization 2 it can be observed that the DTP of $LP_{0,6}$, $LP_{0,5}$, $LP_{0,4}$ and $LP_{0,3}$ is progressively blue shifted at the same time the depth of the attenuation band increases up to 15 dB.

In Fig. 2 numerical and experimental results of LPFG 1 at $LP_{0,6}$ DTP and LPFG 2 at $LP_{0,3}$ DTP are shown. In addition to this, the effective indices as a function of wavelength for LPFG 1 and LPFG 2 are displayed. In LPFG 2, with a lower diameter, there is a higher separation. Two surrounding refractive indices have been analyzed: 1.0 and 1.413. The variation in the effective index is higher for the cladding modes of LPFG 2. The most interesting point is that even $LP_{0,6}$ in LPFG 2 experiences a higher variation than $LP_{0,6}$ in LPFG 1. In other words, the same mode in a structure with a smaller diameter has a higher sensitivity to the refractive index. However, the attenuation bands that can be tracked in the optical spectrum, as the cladding diameter is progressively reduced, belong to lower order modes up to the lowest one $LP_{0,2}$ [14]. It has been verified that the diameter of the optical sensor is so small that, due to bending, it is not possible to track the resonances in a reliable fashion. Consequently, we considered that $LP_{0,3}$ DTP is the lowest order band that can be used for sensing.

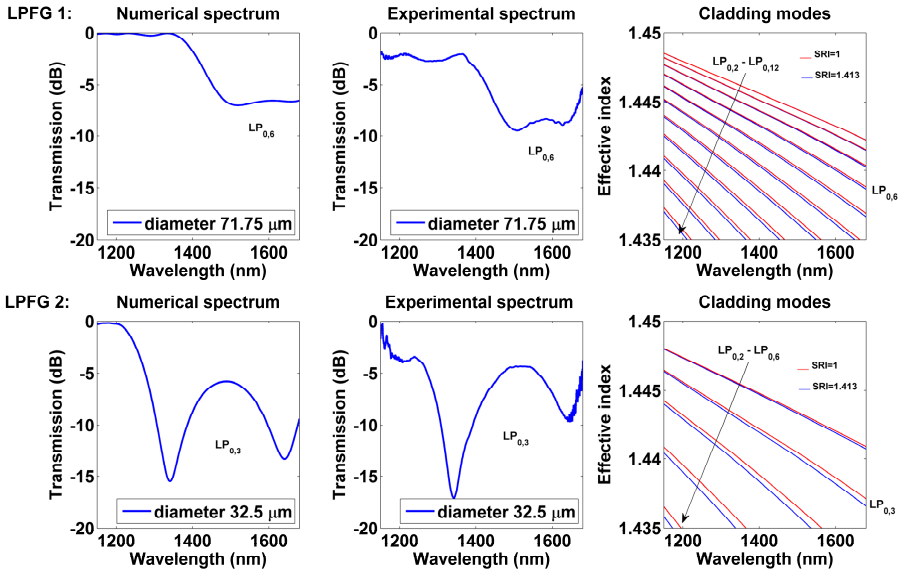

Fig. 2. LPFG 1 etched up to the $LP_{0,6}$ DTP and LPFG 2 up to DTP $LP_{0,3}$: experimental and numerical spectra and cladding mode effective indices for refractive indices 1 and 1.413. In Visualization 1 and in Visualization 2 the etching process up to $LP_{0,6}$ DTP and up to $LP_{0,3}$ DTP is respectively tracked.

After etching, the devices where immersed in the calibrated index solutions indicated in the experimental section. Numerical and experimental spectra as a function of different refractive indices are shown in Fig. 3 for LPFG 1 and LPFG 2 ($LP_{0,3}$ and $LP_{0,6}$ DTP). The lower coupling band experiences a large blue shift with the rising refractive index of the surroundings, whereas the opposite is true for the right coupling band.

Optics EXPRESS

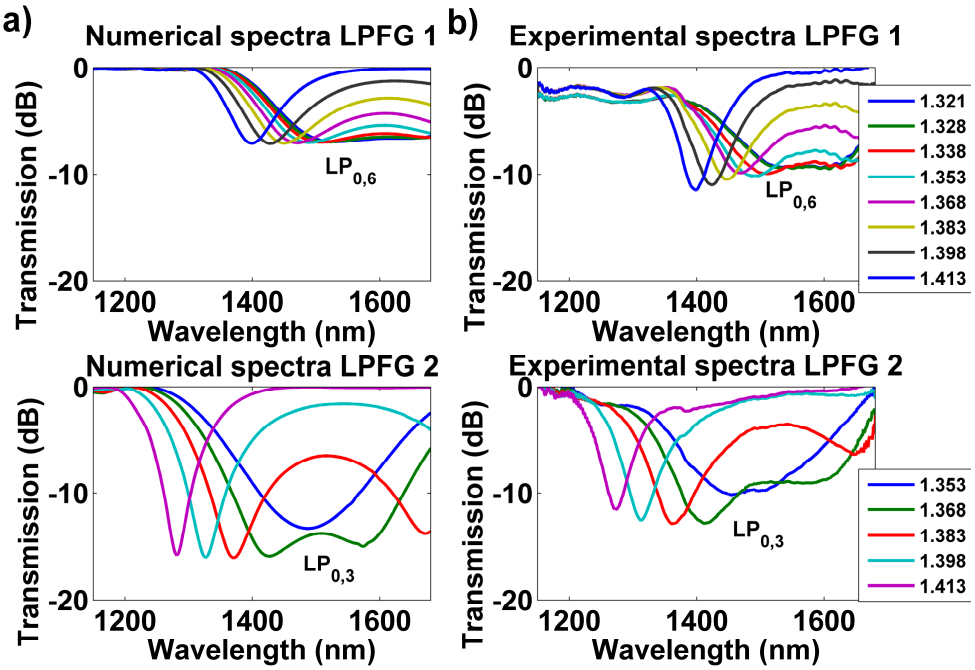

Fig. 3. LPFG 1 and LPFG 2 etched up to the $LP_{0,6}$ DTP and $LP_{0,3}$ DTP. Sensitivity to different refractive indices a) Numerical spectra; b) Experimental spectra.

In order to know the sensitivity to SRI, the response of LPFG 1 and LPFG 2 is shown in Fig. 4(a). LPFG 1 was etched up to the $LP_{0,6}$ band at DTP, whereas LPFG 2 was etched up $LP_{0,3}$ DTP. The left resonance band is represented as function of refractive index. A variation of more than 100 nm can be observed in both cases. The sensitivity in the range 1.353-1398 for $LP_{0,6}$ DTP is 1343 nm/refractive index unit (nm/RIU), whereas the sensitivity for $LP_{0,3}$ DTP improves to 3166 nm/RIU. In the latter case the sensitivity increases by a factor of 2.36 compared to $LP_{0,6}$ DTP. The flat region in the simulations below refractive index 1.36 is due to the fact that both left and right bands in the DTP overlap each other.

The sensitivity can also be analyzed as a function of the separation between the left and right attenuation bands of the DTP [11,13], for those values that can be monitored within the optical spectrum analyzer (see Fig. 4(b)). Since the $LP_{0,3}$ DTP is located at shorter wavelengths it is possible to obtain more points than with $LP_{0,6}$ DTP. This is why only the results of $LP_{0,3}$ are shown. The simulations show that the left and right bands in the DTP overlap each other below a refractive index of 1.36, at this point the separation between the bands is zero.

It is remarkable to say that the sensitivity is 8734 nm/RIU. Moreover, the sensitivity could be enhanced if $LP_{0,2}$ DTP was tracked [14], as it was indicated above.

The sensitivity of 8734 nm/RIU obtained here improves the results of Ref. 11 (1309 nm/RIU in the range 1.333–1.393) and Ref. 13 (1847 nm/RIU in the range 1.335 to 1.360) by a factor of 6.7 and 4.7 respectively, and is similar to the 9100 nm/RIU giant sensitivity obtained with a thin-film coating in [9].

Optics EXPRESS

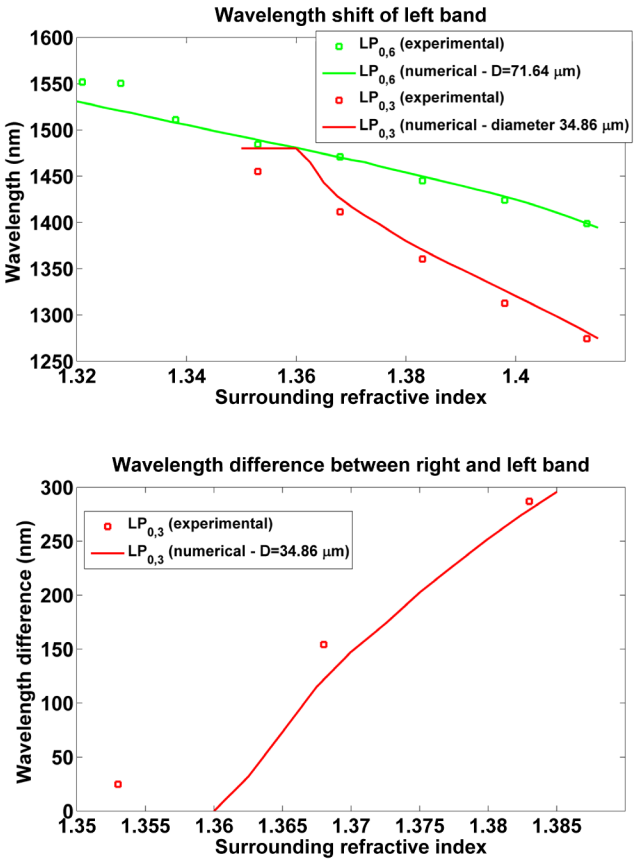

Fig. 4. a) Wavelength shift of the left attenuation band for one LPFG etched up to the $LP_{0,6}$ DTP and for another LPFG etched up to the $LP_{0,3}$ DTP. b) Wavelength difference of bands in LPFG etched up to the $LP_{0,3}$ DTP. Numerical and experimental results are shown.

4. Conclusion

In this work it has been proved that it is possible optimize and increase the sensitivity of uncoated LPFG devices to similar values to those obtained with coating just by combining two phenomena: the dispersion turning point and the cladding etching technique. The results presented here overcome those obtain by a soft-etching of the cladding by more than a factor of four. In addition to this, the length of the device has been adequately selected in order to obtain an optimized coupling to low order cladding modes at the final diameter of the LPFG after etching. We believe the devices presented here will find application in important fields such as biological, chemical or environmental parameter detection.

Acknowledgments

This work was supported in part by the Spanish Ministry of Education and Science-FEDER TEC2013-43679-R. J.L. Cruz also acknowledges financial support of project TEC2013-46643-C2-1-R, and the Generalitat Valenciana project PROMETEOII/2014/072.